Computer Physics Communications 182 (2011) 1995–1998

Contents lists available at ScienceDirect

Computer Physics Communications

www.elsevier.com/locate/cpc

Faddeev Random Phase Approximation for molecules

Matthias Degroote [a,*], Dimitri Van Neck [a], Carlo Barbieri [b]

[a] Center for Molecular Modeling, Ghent University, Technologiepark 903, B-9052 Zwijnaarde, Belgium
[b] Department of Physics, Faculty of Engineering and Physical Sciences, University of Surrey, Guildford GU2 7XH, United Kingdom

ARTICLE INFO

Article history:
Received 30 July 2010
Received in revised form 22 October 2010
Accepted 25 October 2010
Available online 28 October 2010

Keywords:
Quantum chemistry
Green's function
RPA
FRPA

ABSTRACT

The Faddeev Random Phase Approximation is a Green's function technique that makes use of Faddeev-equations to couple two-particle–one-hole and two-hole–one-particle excitations to the single-particle spectrum. Solving these equations implies an infinite partial summation of the perturbation expansion of the self energy. This method goes beyond the third-order Algebraic Diagrammatic Approximation by treating both the particle–hole and particle–particle interactions at the Random Phase Approximation-level. This paper presents the first results of our calculations for diatomic molecules.

1. Introduction

The study of electron correlation by means of first-principle calculations has taken a high rise thanks to modern computer technology. The Green's function formalism is one of these first-principles methods that has successfully been applied in quantum chemistry [1–4]. The correlations in a many-body system are described by an energy dependent self energy. A particular third-order approximation scheme to the self energy is the Algebraic Diagrammatic Construction (ADC) [5] developed by Schirmer and coworkers. This method has proven very successful in predicting electron properties in molecules [6]. This method is equivalent with resumming all two-particle–one-hole (2p1h) and two-hole–one-particle (2h1p) interactions up to Tamm–Dancoff (TDA) level. It has proven very difficult to go beyond the TDA-level [7], even though it is known that the Random Phase Approximation (RPA) should be better to describe long range correlations. The Faddeev Random Phase Approximation (FRPA) [8] solves this problem by using the Faddeev technique to include RPA-phonons in the self energy. This method has successfully been applied to nuclei [9] and atoms [10]. In the first section of this work we will give a short overview of the working equations for the FRPA method. In Section 3 we will present the numerical results for a set of diatomic molecules.

2. Theory

2.1. Single-particle Green's function

The behavior of an electronic many-body system is governed by the Hamiltonian

$$\hat{H} = \sum_{\alpha,\beta} T_{\alpha,\beta} a_\alpha^\dagger a_\beta + \frac{1}{4} \sum_{\alpha,\beta,\gamma,\delta} V_{\alpha\beta,\gamma\delta} a_\alpha^\dagger a_\beta^\dagger a_\delta a_\gamma, \tag{1}$$

where a_α ($a_\alpha^\dagger$) is the annihilation (creation) operator for a state with quantum numbers α and where $T_{\alpha,\beta}$ and $V_{\alpha\beta,\gamma\delta}$ are the matrix elements of the one-body operator and the antisymmetrized two-body operator respectively. For the present study, the one-body operator T represents the kinetic energy and the attraction to the nuclei and V is the Coulomb repulsion between the electrons. The evolution of this N-body system can be described by the single-particle propagator [11]

$$G_{\alpha,\beta}(t,t') = -\frac{i}{\hbar}\langle \Psi_0^N | \mathcal{T}\left[a_\alpha(t) a_\beta^\dagger(t')\right] | \Psi_0^N \rangle, \tag{2}$$

where $\mathcal{T}[\ldots]$ represents the time ordering operator and $a_\alpha(t)$ and $a_\alpha^\dagger(t)$ are the addition and removal operators in the Heisenberg picture. For practical calculations, the Lehmann representation of the Green's function

$$G_{\alpha,\beta}(E) = \sum_{m>F} \frac{\langle \Psi_0^N | a_\alpha | \Psi_m^{N+1} \rangle \langle \Psi_m^{N+1} | a_\beta^\dagger | \Psi_0^N \rangle}{E - (E_m^{N+1} - E_0^N) + i\eta} + \sum_{m<F} \frac{\langle \Psi_0^N | a_\alpha^\dagger | \Psi_m^{N-1} \rangle \langle \Psi_m^{N-1} | a_\beta | \Psi_0^N \rangle}{E - (E_0^N - E_m^{N-1}) - i\eta} \tag{3}$$

* Corresponding author.
E-mail address: matthias.degroote@ugent.be (M. Degroote).

0010-4655/$ – see front matter
doi:10.1016/j.cpc.2010.10.024

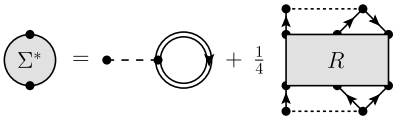

Fig. 1. The Feynman-diagram for the irreducible self energy Σ^* in Eq. (5) within the Faddeev Random Phase Approximation.

is more convenient. This transition to the energy domain transforms the Dyson-equation from an integral equation into the matrix relation

$$G_{\alpha,\beta}(E) = G^{(0)}_{\alpha,\beta}(E) + \sum_{\gamma,\delta} G^{(0)}_{\alpha,\gamma}(E)\Sigma^*_{\gamma,\delta}(E)G_{\delta,\beta}(E). \tag{4}$$

In this equation the fully consistent Green's function G is given in terms of its non-interacting form $G^{(0)}$ and the irreducible self energy Σ^*. Approximation schemes for the single-particle Green's function boil down to finding an appropriate perturbation expansion for the irreducible self energy. In our approach, we want to couple the single-particle states with 2p1h and 2h1p states. The irreducible self energy can be expanded as (Fig. 1)

$$\Sigma^*_{\alpha,\beta}(E) = \Sigma^{HF}_{\alpha,\beta} + \frac{1}{4}\sum_{\lambda,\mu,\nu}\sum_{\epsilon,\theta,\sigma} U_{\alpha\nu,\lambda\mu}R_{\lambda\mu\nu,\epsilon\theta\sigma}(E)U_{\epsilon\theta,\beta\sigma}, \tag{5}$$

where U is the modified antisymmetrized two-particle interaction.

$$U_{\alpha\beta,\gamma\delta} = \sum_{\lambda,\mu}(\mathbb{1}_{\alpha\beta,\lambda\mu} + \Delta U_{\alpha\beta,\lambda\mu})V_{\lambda\mu,\gamma\delta}. \tag{6}$$

This ΔU is needed to guarantee full summation up to third order perturbation theory and was found to be the same as the vertex correction used in the third order Algebraic Diagrammatic Construction (ADC(3)) [5]. The object $R(E)$ in Eq. (5) represents the approximate propagator in 2p1h/2h1p space.

2.2. pp/ph RPA interaction

We want to include particle–particle (pp) and particle–hole (ph) interactions that are correct up to the random phase approximation level. This approximation allows for a dynamic screening of the Coulomb interaction. The pp and ph interactions Γ^{pp} and Γ^{ph} will be used as building blocks for the 2p1h and 2h1p interaction (Figs. 1 and 2). They can be derived from the RPA-equation (Fig. 2) for the pp propagator [12]

$$G^{pp}_{\alpha\beta,\gamma\delta}(E) = G^{pp(0)}_{\alpha\beta,\gamma\delta}(E) + G^{pp(0)}_{\alpha\beta,\alpha\beta}(E)\Gamma^{pp}_{\alpha\beta,\gamma\delta}(E)G^{pp(0)}_{\gamma\delta,\gamma\delta}(E) \tag{7}$$

$$= \sum_m \frac{\mathcal{X}^{pp}_{\alpha\beta,m}\mathcal{X}^{pp\dagger}_{\gamma\delta,m}}{E-\epsilon^{pp+}_m+i\eta} - \sum_n \frac{\mathcal{Y}^{pp}_{\gamma\delta,n}\mathcal{Y}^{pp\dagger}_{\alpha\beta,n}}{E-\epsilon^{pp-}_n-i\eta}, \tag{8}$$

and the ph polarization propagator

$$\Pi^{ph}_{\alpha\beta,\gamma\delta}(E) = \Pi^{ph(0)}_{\alpha\beta,\gamma\delta}(E) + \Pi^{ph(0)}_{\alpha\beta,\alpha\beta}(E)\Gamma^{ph}_{\alpha\beta,\gamma\delta}(E)\Pi^{ph(0)}_{\gamma\delta,\gamma\delta}(E) \tag{9}$$

$$= \sum_m \frac{\mathcal{X}^{ph}_{\alpha\beta,m}\mathcal{X}^{ph\dagger}_{\gamma\delta,m}}{E-\epsilon^{ph+}_m+i\eta} - \sum_n \frac{\mathcal{Y}^{ph\dagger}_{\alpha\beta,n}\mathcal{Y}^{ph}_{\gamma\delta,n}}{E-\epsilon^{ph-}_n-i\eta}. \tag{10}$$

The actual calculation of the amplitudes and poles of the pp propagator and ph polarization propagator can be done by solving the generalized eigenvalue problems.

2.3. Faddeev equations

The diagrammatic content of R cannot be cast into a Bethe–Salpeter equation without double counting of some classes of diagrams. That is why we use the Faddeev technique [13]: to split these objects into three parts. The analysis will be done for R^{2p1h} so that first two indices indicate states above the Fermi-level and the last indicates a state below the Fermi-level. The derivation of R^{2h1p} is found to be completely analogous, but with an interchange of particle and hole states.

$$R^{2p1h}_{\alpha\beta\gamma,\lambda\mu\nu}(E) = G^{(0)>}_{\alpha\beta\gamma,\lambda\mu\nu}(E) - G^{(0)>}_{\alpha\beta\gamma,\mu\lambda\nu}(E) + \sum_{i=1,2,3} R^{(i)}_{\alpha\beta\gamma,\lambda\mu\nu}(E), \tag{11}$$

where the $G^{(0)>}$ is the part of the non-interacting 2p1h propagator which propagates a positive energy:

$$G^{(0)>}_{\alpha\beta\gamma,\lambda\mu\nu}(E) = \frac{\delta_{\alpha\lambda}\delta_{\beta\mu}\delta_{\gamma\nu}}{E-(\epsilon_\alpha+\epsilon_\beta-\epsilon_\gamma)+i\eta}. \tag{12}$$

Each propagator $R^{(i)}$ ends with lines j and k interacting through the adequate RPA interaction vertex, while all possible prior interactions are included in $R^{(j)}$, $R^{(k)}$ and the non-interacting propagators. The inclusion of prior interactions introduces a connection between the different $R^{(i)}$. The Bethe–Salpeter equations (Fig. 3)

$$R^{(i)}_{\alpha\beta\gamma,\lambda\mu\nu}(E) = \sum_{\zeta\eta,\theta}\left(G^{(0)>}\Gamma^{(i)}\right)_{\alpha\beta\gamma,\zeta\eta\theta}(E)\left(G^{(0)>}_{\zeta\eta\theta,\lambda\mu\nu}(E) - G^{(0)>}_{\zeta\eta\theta,\mu\lambda\nu}(E) + R^{(j)}_{\zeta\eta\theta,\lambda\mu\nu}(E) + R^{(k)}_{\zeta\eta\theta,\lambda\mu\nu}(E)\right) \tag{13}$$

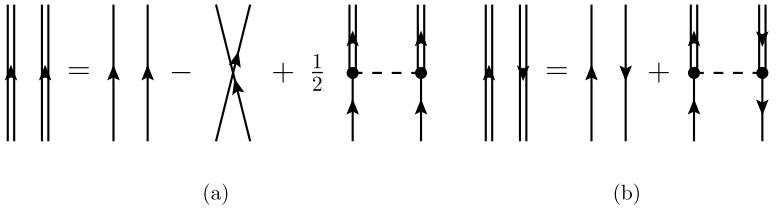

Fig. 2. The diagrammatical representation of the pp-RPA equation (a) and the ph-RPA equation (b) where the dashed line is the antisymmetric interaction and single lines represent non-interacting and the double lines interacting propagators.

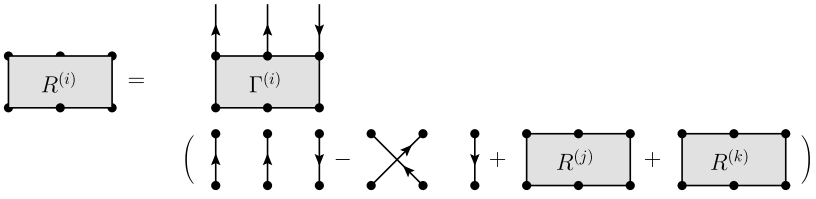

Fig. 3. Diagrammatic representation of Eq. (12).

form a closed self-consistent system. The Lehmann representation for $R^{(i)}$

$$R^{(i)}_{\alpha\beta\gamma,\lambda\mu\nu} = \sum_m \frac{\mathcal{X}^{(i)}_{\alpha\beta\gamma,m}\mathcal{X}_{\lambda\mu\nu,m}}{E-\epsilon^{Fd}+i\eta} + R^{(i)free}_{\alpha\beta\gamma,\lambda\mu\nu} \tag{14}$$

is used as the definition of the poles ϵ^{Fd}_m and residues $\mathcal{X}^{(i)}_{\alpha\beta\gamma,m}$. The part corresponding to uncorrelated poles is gathered in $R^{(i)free}$. The spectroscopic amplitude can be recovered by summing over the three Faddeev components

$$\mathcal{X}_{\alpha\beta\gamma,m} = \sum_{i=1,2,3} \mathcal{X}^{(i)}_{\alpha\beta\gamma,m}. \tag{15}$$

By multiplying Eq. (14) with $(E-\epsilon^{Fd}_m)$ and taking the limit for $E\to\epsilon^{Fd}_m$, the problem is reduced to an eigenvalue problem for the spectroscopic amplitudes and the poles. The uncorrelated poles don't coincide with the Faddeev-poles, so the $R^{(i)free}$ is guaranteed to disappear when taking the limit:

$$\mathcal{X}^{(i)}_{\alpha\beta\gamma,m} = \sum_{\zeta<\eta,\theta} \left(G^{(0)>}\Gamma^{(i)}\right)_{\alpha\beta\gamma,\eta\zeta\theta}\left(\epsilon^{Fd}_m\right)\left(\mathcal{X}^{(j)}_{\eta\zeta\theta,m}+\mathcal{X}^{(k)}_{\eta\zeta\theta,m}\right). \tag{16}$$

When substituted in Eq. (16), this has the structure

$$\mathcal{X}^{(i)} = \left(U^{(i)}\frac{1}{\epsilon^{Fd}_m - D^{(i)}}T^{(i)\dagger} + H^{(i)}H^{(i)\dagger}\right)\left(\mathcal{X}^{(j)}+\mathcal{X}^{(k)}\right). \tag{17}$$

The vectors $U^{(i)}$, $D^{(i)}$, $T^{(i)}$ and $H^{(i)}$ are all diagonal in the freely propagating line and can be written in terms of the pp- and ph-amplitudes and energies, see Ref. [8] for their explicit form. By introducing a vector containing these three components:

$$X = \begin{pmatrix}\mathcal{X}^{(1)}\\ \mathcal{X}^{(2)}\\ \mathcal{X}^{(3)}\end{pmatrix}. \tag{18}$$

This non-linear equation in the Faddeev-energies and amplitudes can be written in the form

$$X = \left(U\frac{1}{\epsilon^{Fd}-D}T^{\dagger} + HH^{\dagger}\right)MX, \tag{19}$$

where the matrix M

$$M = \begin{pmatrix}0 & \mathbb{1} & \mathbb{1}\\ \mathbb{1} & 0 & \mathbb{1}\\ \mathbb{1} & \mathbb{1} & 0\end{pmatrix} \tag{20}$$

takes care of the coupling between the different channels. After some matrix algebra, this can be converted into a non-hermitian eigenvalue problem

$$\epsilon^{Fd}X = \left(\mathbb{1}-HH^{\dagger}M\right)^{-1}U\left[T^{\dagger}M + DU^{-1}\left(\mathbb{1}-HH^{\dagger}M\right)\right]X. \tag{21}$$

The matrix dimensions of the eigenvalue problem are three times the size of the 2p1h basis.

2.4. Handling spurious solutions

The use of Faddeev-equations naturally introduces spurious solutions. The solutions for which the sum in Eq. (15) is zero, have no physical meaning and have to be discarded. At the same time the vectors themselves will have to be antisymmetric under exchange of the two particle or hole lines. By projecting the Hamiltonian matrix (21) onto the vector that has the right symmetry properties and is non-vanishing when summed the matrix dimensions will be reduced by a factor of 3. This vector space is spanned by the vector

$$\frac{1}{\sqrt{6}}\begin{pmatrix}\mathbb{1}-\mathbb{1}_{ex}\\ \mathbb{1}-\mathbb{1}_{ex}\\ \mathbb{1}-\mathbb{1}_{ex}\end{pmatrix}, \tag{22}$$

where $(\mathbb{1}_{ex})_{\alpha\beta\gamma,\lambda\mu\nu} = \delta_{\alpha\mu}\delta_{\beta\lambda}\delta_{\gamma\nu}$. The dimension of the matrix is now the same as in the classic ADC(3) matrix problem. It can be verified that by using Tamm–Dancoff (TDA) interactions and performing this projection, one regains the ADC(3) equations.

2.5. Single-particle propagator and ground-state properties

The calculation of the 2p1h and 2h1p corrections FRPA is now done by a symmetric diagonalization of the matrix

$$\begin{pmatrix}\epsilon^{p/h} & \tilde{U}^{2p1h} & \tilde{U}^{2h1p}\\ \tilde{U}^{2p1h\dagger} & \epsilon^{2p1h} & 0\\ \tilde{U}^{2h1p\dagger} & 0 & \epsilon^{2h1p}\end{pmatrix}, \tag{23}$$

where the ϵ matrices are diagonal in the single-particle, 2p1h and 2h1p energies respectively and the tilde indicates that the coupling matrix elements are written in the basis that diagonalizes the Faddeev matrices. These calculations result in a new single-particle density matrix n and a corresponding ground-state energy

$$E^N_0 = \frac{1}{2}\left(\sum_{\alpha,\beta}\langle\alpha|T|\beta\rangle n_{\alpha\beta} + \sum_{\alpha}\sum_{n<F}\epsilon_n\mathcal{X}_{\alpha,n}\mathcal{X}^{\dagger}_{\alpha,n}\right), \tag{24}$$

where the last summation runs over the single-particle indices of the eigenvectors $\mathcal{X}$ and eigenvalues ϵ beneath the Fermi-level, calculated in the diagonalization of matrix (23). It is also possible to improve the self-consistency of the solution by partial resummation of the Hartree–Fock diagram. Instead of the diagonal matrix of single-particle energies, the Hartree–Fock self energy calculated with the new density matrix n has to be included in the diagonalization.

3. Results and discussion

The accuracy of the FRPA method is evaluated by comparing with the ADC(3) method and Coupled Cluster with Single, Double and perturbative Triple (CCSD(T)) [14] excitations. This method should be of a comparable level of theory as both the ADC(3) and FRPA. All calculations are performed in a correlation-consistent polarized Valence Double Zeta (cc-pVDZ) [15] basis-set. Where possible, the comparison with experimental results [16] is made.

We have calculated the ground-state energies and ionization energies in equilibrium for a set of diatomic molecules with a singlet ground state. A number of different separation distances was calculated around the equilibrium distance, after which a third order polynomial was fitted to find the energy minimum. The results are presented in Tables 1 and 2. The ground-state energies of the molecules with hydrogen show almost no difference between ADC(3) and FRPA. This is to be expected since the difference between the TDA and the RPA interactions is most pronounced for extended systems. The differences for the 14-electron molecules in Table 2 are of the order of 10 milli-Hartree, which is also the accuracy one can expect from the ADC(3) method [6]. The ground-state energies are very close to the CCSD(T) result. The equilibrium bond distances differ more. The equilibrium bond distances for both ADC(3) and FRPA seem to be closer to the experimental value than the CCSD(T) results. In general the deviations from experiment are of the same order for ADC(3) and FRPA. The same conclusion can be made for the ionization energies. One remarkable fact is the lack of an equilibrium state for N_2 in both the ADC(3) and FRPA calculations without self-consistency on the Hartree–Fock level. This example stresses the importance of a consistent treatment of

Table 1
FRPA results for some diatomic molecules in a cc-pVDZ basis-set. E_0 and I in Hartree, r_0 in Å. FRPA and FTDA refer to the calculations after the first iteration, while FRPAc and FTDAc refer to the calculations where consistency on the Hartree–Fock level was applied. The calculated data are compared to the high-level ab-initio method CCSD(T) where available and to experimental data from Ref. [16].

		FTDA	FTDAc	FRPA	FRPAc	CCSD(T)	Expt.
H_2	E_0	−1.170	−1.161	−1.170	−1.161	−1.164	–
	r_0	0.769	0.757	0.770	0.757	0.761	0.741
	I	0.594	0.589	0.594	0.589	0.583	–
HF	E_0	−100.175	−100.224	−100.173	−100.228	−100.228	–
	r_0	0.904	0.916	0.897	0.913	0.920	0.917
	I	0.577	0.577	0.572	0.571	0.628	0.592
HCl	E_0	−460.295	−460.256	−460.293	−460.258	−460.254	–
	r_0	1.314	1.297	1.314	1.293	1.290	1.275
	I	0.457	0.450	0.457	0.450	0.471	
BeH_2	E_0	−15.855	−15.831	−15.856	−15.832	−15.835	–
	r_0	2.747	2.674	2.766	2.674	2.678	2.680
	I	0.437	0.433	0.435	0.432	0.446[a]	–

[a] Only available at Coupled Cluster with Double excitations (CCD) level.

Table 2
FRPA results for some diatomic molecules in a cc-pVDZ basis-set. E_0 and I in Hartree, r_0 in Å. FRPA and FTDA refer to the calculations after the first iteration, while FRPAc and FTDAc refer to the calculations where consistency on the Hartree–Fock level was applied. The calculated data are compared to the high-level ab-initio method CCSD(T) where available and to experimental data from Ref. [16].

		FTDA	FTDAc	FRPA	FRPAc	CCSD(T)	Expt.
N_2	E_0	–	−109.258	–	−109.272	−109.276	–
	r_0	–	1.104	–	1.106	1.119	1.098
	I	–	0.565	–	0.544	0.602[a]	0.573
BF	E_0	−124.331	−124.365	−124.332	−124.368	−124.380	–
	r_0	1.285	1.284	1.305	1.285	1.295	1.267
	I	0.417	0.395	0.431	0.402	0.406	–
CO	E_0	−113.096	−113.037	−113.100	−113.048	−113.055	–
	r_0	1.140	1.130	1.133	1.123	1.145	1.128
	I	0.529	0.503	0.523	0.494	0.550[a]	0.515

[a] Only available at CCD level.

the static self energy. The inclusion of self-consistency in the calculations tends to adjust the results in the right direction where needed compared to the experiment.

4. Conclusion

In this work we have successfully applied the FRPA technique to a set of diatomic molecules. The computational cost of this method is not much higher than for the more established ADC(3) method and in any case lower than for CCSD(T). The results are comparable in accuracy to the ones obtained with the ADC(3) method. The difference between the two methods is larger for more extended systems due to the nature of the RPA phonons. The possibility of complex eigenvalues in the RPA and FRPA eigenvalue equations is a problem that has to be kept in mind. The self-consistent treatment of the Hartree–Fock diagram has a positive effect on the numerical results and should always be included.

Acknowledgement

This research is supported by a Ph.D. fellowship of the Flemish Research Foundation (FWO).

References

[1] J. Linderberg, Y. Öhrn, Propagators in Quantum Chemistry, Academic, London, 1973.
[2] L.S. Cederbaum, W. Domcke, Adv. Chem. Phys. 36 (1977).
[3] W. Vonniessen, J. Schirmer, L. Cederbaum, Comput. Phys. Rep. 1 (1984) 57.
[4] J.V. Ortiz, The Electron Propagator Picture of Molecular Electronic Structure, vol. 2, World Scientific, Singapore, 1997.
[5] J. Schirmer, L.S. Cederbaum, O. Walter, Phys. Rev. A 28 (1983).
[6] M.S. Deleuze, M.G. Giuffreda, J.-P. François, L.S. Cederbaum, J. Chem. Phys. 111 (1999) 5851.
[7] G.A. Rijsdijk, W.J.W. Geurts, K. Allaart, W.H. Dickhoff, Phys. Rev. C 53 (1996).
[8] C. Barbieri, W.H. Dickhoff, Phys. Rev. C 63 (2001) 034313.
[9] C. Barbieri, W.H. Dickhoff, Phys. Rev. C 65 (2002) 064313.
[10] C. Barbieri, D. Van Neck, W.H. Dickhoff, Phys. Rev. A 76 (2007) 052503.
[11] W.H. Dickhoff, D.V. Neck, Many Body Theory Exposed! 2nd edition, World Scientific, Singapore, 2008.
[12] P. Ring, P. Schuck, The Nuclear Many-Body Problem, Springer-Verlag, New York, 1980.
[13] L.D. Faddeev, Israel Program for Scientific Translations, 1965.
[14] K. Raghavachari, G.W. Trucks, J.A. Pople, M. Head-Gordon, Chemical Physics Letters 157 (1989) 479.
[15] T.H. Dunning Jr., J. Chem. Phys. 90 (1989) 1007.
[16] NIST Computational Chemistry Comparison Benchmark Database, NIST Standard Reference Database Number 101 Release 15a, http://cccbdb.nist.gov/, 2010.